Solvent Effect on the Sensitized Photooxygenation of 2,3-Dihydropyrazine Derivatives

Else Lemp,* Antonio L. Zanocco, German Günther, and Nancy Pizarro

Universidad de Chile, Facultad de Ciencias Químicas y Farmacéuticas, Departamento de Química Orgánica y Fisicoquímica, Casilla 233, Santiago-1, Santiago, Chile

elemp@ciq.uchile.cl

Detection of $O_2(^1\Delta_g)$ phosphorescence emission, $\lambda_{max} = 1270$ nm, following laser excitation and steady-state methods was employed to determine the total rate constant, k_T, and the chemical reaction rate constant, k_R, for reaction between 5,6-disubstituted-2,3-dihydropyrazines and singlet oxygen in several solvents. Values of k_T ranged from 0.26×10^5 M^{-1} s^{-1} in hexafluoro-2-propanol to 58.9 $\times 10^5$ M^{-1} s^{-1} in N,N-dimethylacetamide for 5,6-dimethyl-2,3-dihydropyrazine (DMD) and from 5.74×10^5 M^{-1} s^{-1} in trifluoroethanol to 159.0×10^5 M^{-1} s^{-1} in tributyl phosphate for 5-methyl-6-phenyl-2,3-dihydropyrazine (MPD). Chemical reaction rate constants, k_R, for DMD are similar to k_T in polar solvents such as propylencarbonate, whereas for MPD in this solvent, the contribution of the chemical channel to the total reaction is about of 4%. Dependence of the total rate constant on solvent microscopic parameters, α and π^*, for DMD can be explained in terms of a reaction mechanism that involves formation of a perepoxide exciplex. Replacement of the methyl by a phenyl substituent enhances dihydropyrazine ring reactivity toward singlet oxygen and modifies the dependence of k_T on solvent parameters, specially on the Hildebrand parameter. These results are explained in terms of an additional reaction path, involving a perepoxide-like exciplex stabilized by the interaction of the negative charge on the terminal oxygen of the perepoxide with the aromatic π system.

Introduction

Reactions of singlet oxygen, $O_2(^1\Delta_g)$, with olefins proceed through several mechanisms, among them ene-reactions producing hydroperoxide intermediates in molecules with allylic hydrogens; $[4 + 2]$ cycloadditions giving relatively stable or labile endoperoxides, depending on the olefin substitution; and $[2 + 2]$ cycloadditions that mainly yield dioxetane intermediates.[1-4] Extensive work shows that the main process and its dominant pathway in these systems is determined by olefin structure and solvent properties. Furthermore, it has been pointed out that the solvent has only a minor role in determining the total rate of interaction of singlet oxygen with monoolefins or 1,3-dienes.[5] Unlike the extensive studies covering reactions of singlet oxygen with compounds having carbon–carbon double bonds, only very few data are suitable for rationalizing product distribu-

tions in reactions of singlet oxygen with molecules having carbon–nitrogen double bonds.[6-10] The product distribution dependence on temperature and substituents and comparison with the behavior of the alkene homologues indicate that reactions of $O_2(^1\Delta_g)$ with imino compounds involve several intermediates, i.e., dioxazetidines by $[2 + 2]$ concerted cycloaddition to the carbon–nitrogen double bond,[7,8] peroxide ions from electrophilic attack on iminic carbon,[7] and hydroperoxides from rearrangement of pernitrones in reactions with substituted 2,3-dihydropyrazines.[11] The involvement of pernitrone intermediates in this last reaction is explained through a mechanism in which excited oxygen interacts with the iminic nitrogen lone pair.

From these studies it is not possible to decide whether imino group reactivity toward singlet oxygen is similar

---

* Corresponding author. Phone: 56-2-6782877. Fax: 56-2-6782868.

(1) Clennan, E. L. *Tetrahedron* **1991**, *47*, 1343–1382.

(2) Frimer, A. *Chem. Rev.* **1979**, *79*, 359–387.

(3) Prein, M.; Adam, W. *Angew. Chem., Int. Ed. Engl.* **1996**, *35*, 477–494.

(4) Stratakis, M.; Orfanopoulus, M. *Tetrahedron* **2000**, *56*, 1595–1615.

(5) Lissi, E. A.; Encinas, M. V.; Lemp, E.; Rubio, M. A. *Chem. Rev.* **1993**, *93*, 699–723.

(6) George, M. V.; Bhat, V. *Chem. Rev.* **1979**, *79*, 447–478.

(7) Ito, Y.; Kyono, K.; Matsuura, T. *Tetrahedron Lett.* **1979**, 2253–2256.

(8) Vaidya, V. K. *J. Photochem. Photobiol. A: Chem.* **1994**, *81*, 135–137.

(9) Castro, C.; Dixon, M.; Erden, I.; Ergonec, P.; Keeffe, J.; Sukhovistsky, A. *J. Org. Chem.* **1989**, *54*, 3732–3738.

(10) Erden, I.; Griffin, A.; Keeffe, J.; Brinck-Kohn, V. *Tetrahedron Lett.* **1993**, *34*, 793–796.

(11) Gollnick, K.; Koegler, S.; Maurer, D. *J. Org. Chem.* **1992**, *57*, 229–234.
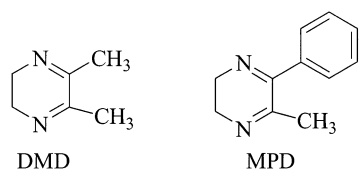
FIGURE 1. Structures of 5,6-dimethyl-2,3-dihydropyrazine (DMD) and 5-methyl-6-phenyl-2,3-dihydropyrazine (MPD).

to that of homologous alkenes or due to the nitrogen heteroatom if the behavior departs significantly from the well-known alkene–singlet oxygen chemistry. In this work we report on reactions of singlet oxygen with 2,3-dihydropyrazine derivatives (Figure 1) including different substituents on the iminic carbon. Our aim is to account for the reaction mechanism both from kinetics, including measurements of rate constants for chemical and physical reaction channels in several solvents, and product characterization. Solvent effects are analyzed in terms of linear solvation energy relationships (LSER)[12,13] and theoretical linear solvation energy relationships (TLSER).[14] These equations give very useful quantitative evaluations of solvent effects and are powerful tools in interpreting mechanisms of such processes.[15−19]

Results

Total Reaction of DMD and MPD with Singlet Oxygen. The total quenching rate constant (physical and chemical), k_T, for reaction of $O_2(^1\Delta_g)$ with the 5,6-disubstituted-2,3-dihydropyrazines DMD and MPD (Figure 1) in several solvents was obtained from the first-order decay of $O_2(^1\Delta_g)$ in the absence (τ_o^{-1}) and presence of dihydropyrazine (τ^{-1}) according to eq 1.

$$\tau^{-1} = \tau_o^{-1} + k_T[\text{dihydropyrazine}] \quad (1)$$

Triplet decay of the sensitizer employed in most solvents (TPP) was not affected by addition of substituted dihydropyrazine, even at concentrations higher than those used to quench excited oxygen. Linear plots of τ^{-1} vs [dihydropyrazine] were obtained in all solvents employed (Figure 2). Intercepts of these plots match closely with reported[20] and measured (in a large number of independent experiments from our laboratory) singlet oxygen lifetimes in the same solvent. For example, the singlet oxygen lifetime in acetone, obtained from data in Figure 2, was 50 μs, very close to the reported value of 51 μs.[20]

(12) Reichardt, C. *Solvents and Solvent Effects in Organic Chemistry*, 2th ed.; VCH: Weinheim, 1990.
(13) Abraham, M.; Doherty, R.; Kamlet, M.; Harris, J. M.; Taft, R. *J. Chem. Soc., Perkin Trans 2* **1987**, 913−920.
(14) Cronce, D. T.; Famini, G. R.; De Soto, J. A.; Wilson, L. Y. *J. Chem. Soc., Perkin Trans. 2* **1998**, 1293−1301.
(15) Zanocco, A. L.; Günther, G.; Lemp, E.; De La Fuente, J. R.; Pizarro, N. *Photochem. Photobiol* **1998**, *68*, 487−493.
(16) Zanocco, A. L.; Lemp, E.; Pizarro, N.; De La Fuente, J. R.; Günther, G. *J. Photochem. Photobiol.* **2001**, *140*, 109−115.
(17) Lemp, E.; Pizarro, N.; Encinas, M. V.; Zanocco, A. L. *Phys. Chem. Chem. Phys.* **2001**, *3*, 5222−5225.
(18) Lissi, E. A.; Lemp, E.; Zanocco, A. L. *Singlet Oxygen Reactions. Solvent and Compartmentalization Effects. Molecular and Supramolecular Photochemistry: Understanding and Manipulating Excited-States Processes*; Ramamurthy V., Schanze, K. S., Ed.; Marcel Dekker Inc.: New York, 2001; Vol 8, Chapter 3.
(19) Lemp, E.; Zanocco, A. L.; Lissi, E. *Curr. Org. Chem.* Submitted.
(20) Wilkinson, F. *J. Phys. Chem. Ref. Data* **1995**, *24*, 663−1021.

FIGURE 2. Stern−Volmer plot for deactivation of singlet oxygen by DMD in acetone. (Inset a) Singlet oxygen phosphorescence decay at 1270 nm, following dye laser excitation at 532 nm, with Rose Bengal as sensitizer in acetone. (Inset b) as in part a, but with 13.6 mM DMD.

TABLE 1. Values of k_T for Reactions of DMD and MPD with $O_2(^1\Delta_g)$ in Different Solvents

		$k_T/10^5$ M^{-1} s^{-1}	
	solvent	DMD	MPD
1	hexafluoro-2-propanol	0.26 ± 0.01	
2	chloroform	2.23 ± 0.13	12.0 ± 0.06
3	trifluoroethanol	3.04 ± 0.16	5.74 ± 0.25
4	*n*-hexane	3.60 ± 0.17	
5	ethanol	3.69 ± 0.19	22.1 ± 0.99
6	*n*-heptane	4.31 ± 0.18	28.9 ± 1.15
7	benzyl alcohol	4.48 ± 0.21	23.3 ± 0.09
8	*n*-butanol	4.94 ± 0.22	
9	methanol	5.23 ± 0.22	26.4 ± 1.15
10	benzene	5.34 ± 0.21	49.5 ± 1.98
11	*n*-pentanol	5.44 ± 0.19	
12	anisole	6.01 ± 0.33	63.0 ± 2.29
13	diethyl ether	6.08 ± 0.31	37.7 ± 1.69
14	benzonitrile	6.25 ± 0.41	41.9 ± 1.65
15	methylene chloride	7.36 ± 0.31	37.1 ± 1.29
16	*n*-propanol	8.60 ± 0.38	25.5 ± 1.09
17	acetonitrile	9.87 ± 0.41	67.3 ± 3.02
18	tetrahydrofuran	12.9 ± 0.48	50.6 ± 2.85
19	ethyl acetate	13.6 ± 0.58	51.6 ± 2.12
20	acetone	13.7 ± 0.43	60.4 ± 2.63
21	dioxane	14.6 ± 0.55	60.8 ± 3.00
22	*N,N*-dimethylformamide	19.3 ± 0.72	101.1 ± 4.19
23	propylencarbonate	20.3 ± 0.89	68.1 ± 3.27
24	tributyl phosphate	56.8 ± 2.34	159.0 ± 4.38
25	*N,N*-dimethylacetamide	58.9 ± 2.61	

Values of k_T calculated from slopes of these plots are given in Table 1 and were independent of the laser pulse energy (between 2 and 5 mJ). Possible rapid chemical changes of samples during illumination or interference of the $O_2(^1\Delta_g)$ luminescence with the scattered laser light and the tail end of the sensitizer fluorescence[21] can be disregarded, since the rate constant measured in some solvents (data not shown) by using competitive steady-state methods, such as the inhibition of the autoxidation rate of rubrene ($\lambda_{max} = 520$ nm)[22] or by following the consumption rate of 9,10-dimethylanthracene in absence

(21) Michaeli, A.; Feitelson, J. *Photochem. Photobiol.* **1994**, *59*, 284−288.
(22) Carlson, D. J.; Mendenhall, E. D.; Suprunchuk, T.; Wiles, D. M. *J. Am. Chem. Soc.* **1972**, *94*, 8960−8963.

and presence of dihydropyrazine derivatives,[23] afforded the same value as that obtained by time-resolved experiments.

Data in Table 1 show that the total quenching rate constant for reaction of DMD with singlet oxygen increases by more than 2 orders of magnitude when the solvent is changed from hexafluoro-2-propanol to *N,N*-dimethylacetamide. Similarly, MPD rate constants increase by about a factor of 30 on changing from trifluoroethanol to tributyl phosphate. Also, we found for all solvents that the total rate constants for MPD are near to 1 order of magnitude larger than those for DMD. As expected, these results show that dihydropyrazines behave similarly to related olefins and reactivities toward singlet oxygen depend on both dihydropyrazine structure and solvent properties. However, solvent effects are larger than those for diolefins[5] and cannot be associated only with changes in macroscopic properties such as dielectric constant, suggesting the existence of specific solute−solvent interactions. We have previously demonstrated that in these cases it is useful to use linear solvent free-energy relationships to correlate experimental rate constants with solvent properties.[15−19]

Therefore, to obtain insights on solvent effects on interactions of singlet oxygen with dihydropyrazines, we analyze the quenching rate constant dependence on microscopic solvent parameters by using the semiempirical solvatochromic equation (LSER) of Kamlet et al. (eq 2).[12,24]

$$\log k = \log k_0 + s\pi^* + d\delta + a\alpha + b\beta + h\rho_H{}^2 \quad (2)$$

where π^* accounts for polarizabilities and dipolarities of solvents;[25−27] δ is a correction term for polarizability; α is related to the hydrogen-bond donor solvent ability; β indicates solvent capability as a hydrogen-bond acceptor; and ρ_H is the Hildebrand parameter, which corresponds to the square root of solvent cohesive density and is a measure of disruption of solvent−solvent interactions in creating a cavity.[12,28] Also, we analyzed the dependence of k_T on solvent by using a theoretical set of correlation parameters determined solely from computational methods.[14,29,30] The theoretical linear solvation relationship (TLSER) descriptors have been developed to give optimal correlation with LSER descriptors.[14,29] The generalized TLSER equation proposed by Famini et al.[14,29] (eq 3) can be used to analyze dependence of reaction rates on solvent properties.

$$\log k = \log k_0 + s\pi_1 + b\epsilon_b + cq_- + d\epsilon_a + eq_+ + h\rho_H{}^2 \quad (3)$$

In eq 3, the bulk/steric term is described by the Hildebrand parameter, ρ_H. The parameter π_1 corresponds to the index of polarizability, accounts for the ease of moving or polarizing the electron cloud, and is obtained from the ratio between polarizability volume and molecular volume. The hydrogen bond acceptor basicity (HBA) involves covalent, ϵ_b, and electrostatic, q_-, terms. Similarly, hydrogen-bond donor acidity (HBD) includes covalent, ϵ_a, and electrostatic, q_+, terms.[29,31]

The coefficients of the LSER and TLSER equations (eqs 2 and 3) obtained by multilinear correlation analysis for dependence of k_T on solvent parameters are given in Table 2 and are based on purely statistical criteria. Current criteria used for derivation of the correlation equations include the following: (a) Descriptor coefficients accepted in the correlation equation are those that have a significance level ≥0.95 [large *t*-statistic, P(two-tail) < 0.05]. (b) The VIF statigraph,[32] a measure of parameter orthogonality that indicates independence of the parameters, is defined by VIF $= 1/(1 - R^2)$, where R is the correlation coefficient for that particular parameter in terms of the other parameters. For a given parameter, the closer VIF is to unity, the less cross-correlation there is with the other parameters. When VIF is too large, the least significant variable is eliminated. We accept a low variable collinearity (VIF < 5). (c) The correlation coefficient, R, is equal to or higher than 0.90 (variance, $R^2 > 0.80$). (d) The sample size is as large as possible; N must be at least three times the number of independent parameters included in the correlation equation. In summary, the sample size, N, the product correlation coefficient, R, the standard deviation, SD, and the Fisher index of equation reliability, F, indicate the quality of the overall correlation equation. The reliability of each term is indicated by the *t*-statistic (*t*-stat) and the variance inflation factor (VIF). Good quality is indicated by large N, F, and *t*-stat values; small SD values; and R and VIF close to 1.

Results in Table 2 show that not all descriptors are important. Descriptor coefficients accepted in the correlation equation were those that have a significance level ≥0.95. For this reason ρ_H and π^* parameters were not included in the LSER correlation for DMD and MPD, respectively. According to the LSER coefficients in Table 2, k_T values for DMD increase in solvents with the largest capacities to stabilize charges and dipoles and decrease in strong HBD solvents. Furthermore, for MPD rate constants increase in HBA solvents with high cohesive energy and decrease in strong HBD solvents. Similarly, in TLSER equations, only q_- and q_+ were included for DMD and ϵ_b, q_+, and ρ_H for MPD.

Results of TLSER analyses accord with those obtained with LSER equations, showing that for DMD k_T increases in HBA solvents and decreases in HBD solvents, and for MPD the rate constant increases in HBA solvents with high cohesive energy and decreases in HBD solvents.

Chemical Reaction of $O_2(^1\Delta_g)$ with Dihydropyrazines. Irradiation of aerated solutions of DMD or MPD in the presence of TPP or RB, at the wavelength for which

(23) Zanocco, A. L.; Lemp, E.; Günther, G. *J. Chem. Soc., Perkin Trans. 2* **1997**, 1299−1302.

(24) Kamlet, M. J.; Abboud, J. L. M.; Abraham, M. H.; Taft, R. W. *J. Org. Chem.* **1983**, *48*, 2877−2887.

(25) Marcus, Y. *Chem. Soc. Rev.* **1993**, *22*, 409−416.

(26) Barton, A. F. M. *Chem. Rev.* **1975**, *75*, 731−752.

(27) Abraham, M. H.; Doherty, R. M.; Kamlet, M. J.; Harris, J. M.; Taft, R. W. *J. Chem. Soc., Perkin Trans. 2* **1987**, 913−920.

(28) Kamlet, M. J.; Carr, P. W.; Taft, R. W.; Abraham. M. H. *J. Am. Chem. Soc.* **1981**, *103*, 6062−6066.

(29) Famini, G. R.; Penski, C. A.; Wilson, L. Y. *J. Phys. Org. Chem.* **1992**, *5*, 395−408.

(30) Cronce, D. T.; Famini, G. R.; De Soto, J. A.; Wilson, L. Y. http://www.rsc.org/suppdata/perkin2/1998/1293.

(31) Famini, G. R.; Wilson, L. Y. *J. Chem. Soc., Perkin Trans. 2* **1994**, 1641−1650.

(32) Belsley, D. A.; Kuh, E.; Welsch R. E. *Regression Diagnostics. Identifying Influential Data and Sources of Collinearity;* Wiley & Sons: New York, 1980.

TABLE 2. LSER and TLSER Correlation Equations for the Reaction of Singlet Oxygen with DMD and MPD

	log k_o	a	b	s	d	h
			DMD			
coeff	5.577	−0.602	0.439	0.629	−0.406	
±	0.081	0.054	0.125	0.140	0.102	
t-stat	68.802	−11.053	3.507	4.500	−3.964	
P(two-tail)	<0.0001	<0.0001	0.0024	0.0002	0.0008	
VIF		1.006	1.572	1.536	1.808	

N = 24, *R* = 0.956, SD = 0.144, *F* = 50.029

	log k_o	a	b	s	d	h
			MPD			
coeff	6.395	−0.692	0.203			0.003
±	0.056	0.050	0.084			0.001
t-stat	114.69	−13.855	2.430			4.561
P(two-tail)	<0.0001	<0.0001	0.0291			0.0004
VIF		1.613	1.379			2.088

N = 18, *R* = 0.970, SD = 0.075, *F* = 74.475

$$\log k = \log k_o + s\pi_1 + b\epsilon_b + cq_- + d\epsilon_a + eq_+ + h\rho_H^2$$

	log k_o	s	b	c	d	e	h
				DMD			
coeff	5.701			1.862		−3.849	
±	0.078			0.277		0.542	
t-stat	72.630			6.729		−7.102	
P(two-tail)	<0.0001			<0.0001		<0.0001	
VIF	-			1.087		1.087	

N = 20, *R* = 0.900, SD = 0.159, *F* = 36.397

	log k_o	s	b	c	d	e	h
				MPD			
coeff	4.677			12.602		−5.148	0.005
	0.312			2.185		0.538	0.001
t-stat.	14.993			5.767		−9.568	5.830
P(two-tail)	<0.0001			<0.0001		<0.0001	<0.0001
VIF				1.009		2.198	2.212

N = 18, *R* = 0.948, SD = 0.104, *F* = 41.143

TABLE 3. Chemical Reaction Rate Constants, k_R, for Reactions of DMD and MPD with O$_2$($^1\Delta_g$) in Different Solvents

	solvent	$k_R/10^5$ M^{-1} s^{-1} DMD	MPD
1	*n*-hexane	0.06 ± 0.01	
2	*n*-heptane	0.09 ± 0.01	
3	diethyl ether	0.57 ± 0.02	
4	tetrahydrofuran	1.70 ± 0.01	
5	ethanol	3.35 ± 0.02	
6	benzene	5.12 ± 0.03	2.18 ± 0.02
7	acetonitrile	5.26 ± 0.04	2.25 ± 0.02
8	propylencarbonate	21.0 ± 0.09	1.53 ± 0.01

only the sensitizer absorbs, decreases the concentration of the dihydropyrazine derivative, and the reaction rate, *r*, follows a first-order kinetics, eq 4.

$$r = k_R [^1O_2][\text{dihydropyrazine}] = k_{obs}[\text{dihydropyrazine}] \quad (4)$$

Rate constants for chemical O$_2$($^1\Delta_g$) quenching by dihydropyrazine derivatives (k_R) in various solvents, obtained from slopes of first-order plots employing 1,3-diphenylisobenzofuran (DPBF) or 9,10-dimethylanthracene (DMA) as actinometers, are in Table 3.

Eventual quenching of excited states of sensitizers by dihydropyrazine can be disregarded, since singlet or triplet deactivation was not observed under our experimental conditions. Data in Table 3 show that DMD
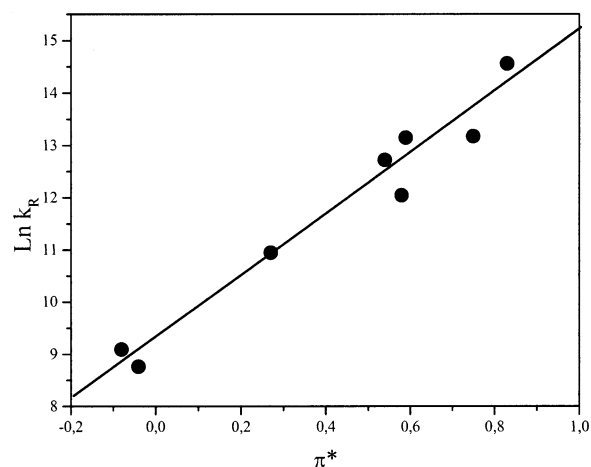
FIGURE 3. Dependence of the chemical reaction rate constant, k_R, for reaction of DMD with singlet oxygen on the solvatochromic parameter π^*.

chemical rate constants are dependent on solvent properties. Thus, in *n*-hexane, the chemical channel of intermediate decomposition is negligible, whereas in more polar solvents, such as ethanol and propylencarbonate, reactive quenching corresponds to the only path for O$_2$($^1\Delta_g$) deactivation. Solvent effects on chemical reaction rate constants cannot be examined in terms of microscopic solvent parameters employing empirical or theoretical linear solvation relationships, given that k_R was
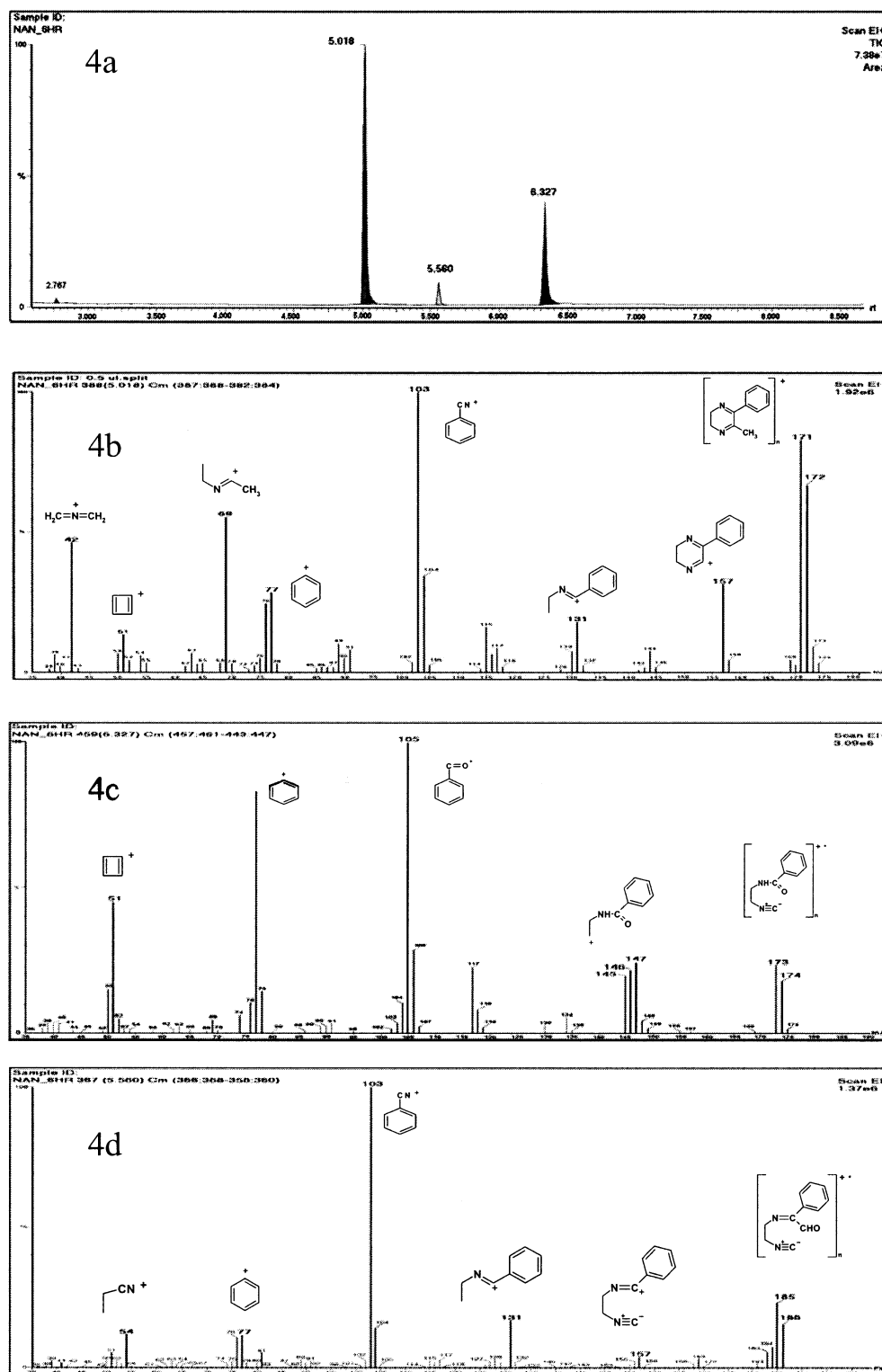
FIGURE 4. (a) GC−MS chromatogram of 1 mM MPD in acetonitrile after 6 h of irradiation in the presence of TPP; (b) EI+ mass spectrum of MPD; (c) EI+ mass spectrum of compound with retention time 6.33 min; (d) EI+ mass spectrum of compound with retention time 5.56 min.

only measured in eight solvents. However, k_R values have an approximate dependence on the solvatochromic parameter π^*, as shown in Figure 3, indicating that in solvents with large π^* values contributions of chemical reactions to the total quenching increase. For MPD, the contribution of the chemical channel to the total quench-ing is minor (about of 4%) in the three solvents employed in measuring k_R. Also, for this compound k_R values were practically independent of the reaction media.

According to Gollnick,[11] dye-sensitized photooxygen-ations of DMP and MPD yield the corresponding 1-iso-cyano-2-(acylamino)ethane and formaldehyde as main

reaction products. We did not attempt to isolate reaction products for spectroscopic characterization, although evidence of product distribution was obtained by GC−MS analysis. When 0.001 M MPD in acetonitrile was irradiated for 6 h in the presence of TPP, the chromatogram shown in Figure 4a was obtained with the mass spectrometer in the electron impact (EI+) operation mode. There were only three major peaks in the chromatogram. Unreacted MPD is the main one with a retention time of 5.02 min. Figure 4b shows that the EI+ mass spectrum is that of MPD. The positive chemical ionization (CI+) (not included) and EI+ mass spectra corresponding to peaks at retention times of 6.33 and 5.56 min indicate that 1-isocyano-2-(benzoylamino)ethane and 1-isocyano-4-phenyl-4-carboxaldehyde-3-aza-3-butene are the probable main products of the photooxidation of MPD. Figure 4c,d shows mass spectra ionization patterns and corresponding structures. Additionally, in a separate experiment in benzene, we confirmed formation of formaldehyde as the photooxidation product by comparison of a signal at retention time of 0.39 min, with that obtained for formaldehyde in benzene.

Analogous reaction products were observed in the photooxidation of DMD. Formaldehyde, 1-isocyano-2-(acylamino)ethane, and 1-isocyano-4-carboxaldehyde-3-aza-3-pentene were the main reaction products.

Discussion

The quenching of singlet oxygen by cyclic α-diimines has been discussed by Gollnick et al.[11] Product distribution was explained in terms of formation of an hydroperoxide intermediate resulting from the rearrangement of a primary reaction intermediate, a "pernitrone" or "nitrone oxide". Other possible reaction pathways, involving interaction of singlet oxygen with C-5 of the dihydropyrazine or addition of $O_2(^1\Delta_g)$ to the C−N double bond giving peroxaziridines, were disregarded on the basis of final product distribution.

Kinetic results obtained in this work indicate that k_T values for singlet oxygen quenching by dihydropyrazines are highly dependent on solvent properties (Table 1). A meaningful interpretation of k_T solvent dependence was obtained by using LSER and TLSER solvatochromic equations. The LSER correlations listed in Table 2 indicate that singlet oxygen reactions with DMD or MPD have different dependence on solvent properties. For DMD, the reaction rate increases in solvents with higher capabilities to stabilize charges and dipoles and decreases in strong hydrogen-bond-donor solvents.

Data are compatible with an exciplex formation with considerable charge separation. This result could be in agreement with formation of both perepoxide and zwitterionic intermediates as proposed by Gollnick et al.[11] (Scheme 1).

However, there are several results supporting formation of a perepoxide as the primary intermediate arising from the interaction between singlet oxygen and DMD. In the LSER equation the coefficient associated with the α parameter is smaller than that generally observed for electrophilic attack of singlet oxygen on a nitrogen lone pair in amino compounds, implying that steric hindrance, due to hydrogen-bonding interactions between strong HBD solvents and the nitrogen atom, inhibits the reac-

SCHEME 1
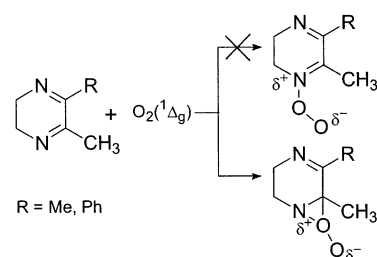
tion but not to the extent observed with tertiary amines.[5,16] This result could be explained if nitrogen is not the reactive center but is close to it. Also, for the same compound we found that the coefficient associated with the π^* parameter is larger than that for reactions of $O_2(^1\Delta_g)$ with amines. In addition, the TLSER treatment shows that HBA solvents assist reaction between singlet oxygen and DMD, whereas HBD inhibits them. Influences of both HBA and HBD solvents are mainly electrostatic, because only the parameters q_- and q_+ are included in the correlation equation. This result can be understood by considering that π_1 is not included in the correlation and it models the solvent's ability to stabilize dipole−induced dipole and induced dipole−induced dipole (dispersive) interactions. No adequate TLSER model for dipolarity itself has been found. The dependence of total reaction rate on the q_+ parameter could be explained if an appreciable charge separation is developed in the N−C double bond. Stabilizing interactions with HBD solvents can sterically block access of singlet oxygen to a reactive bond. Furthermore, if the positive charge on the perepoxide is delocalized throughout the cyclic system formed after singlet oxygen addition, no formal bonding interactions with HBA solvents can be expected. Conversely, there should be electrostatic stabilization of an exciplex by such solvents.

Solvent dependence on k_R for reaction of DMD with $O_2(^1\Delta_g)$ is more significant than that observed for k_T. The chemical rate constant increases by more than 2 orders of magnitude when the solvent is changed from nonpolar (e.g. hexane) to polar (e.g., propylencarbonate). Then, in nonpolar solvents, contribution of the chemical reaction can be considered to be negligible, whereas in polar ones their contribution is the main deactivation channel. Also, it is clear from data in Table 3 and Figure 3 that solvents with large π^* values increase the contribution of the chemical reaction relative to physical quenching. Solvent dependence of k_R can be explained if intermediates along the reaction coordinate have more localized charge than the initial complex. This result is compatible with involvement of ion pairs in controlling the final product distribution, as depicted in Scheme 2.

Values of k_T for reaction of MPD with singlet oxygen are larger than for DMD, and solvent effects are characterized by dependence of k_T on the Hildebrand parameter, as found in both LSER and TLSER analyses. The dependence of the rate constant on the Hildebrand parameter has been ascribed to $O_2(^1\Delta_g)$ reactions that involve a concerted or partially concerted cycloaddition of singlet oxygen to an activated diene.[33] In these reac-

(33) Aubry, J. M.; Mandard-Cazin, B.; Rougee M.; Bensasson, R. *J. Am. Chem. Soc.* **1995**, *117*, 9159−9164.

SCHEME 2
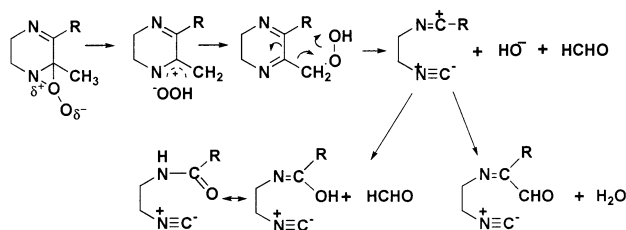
SCHEME 3
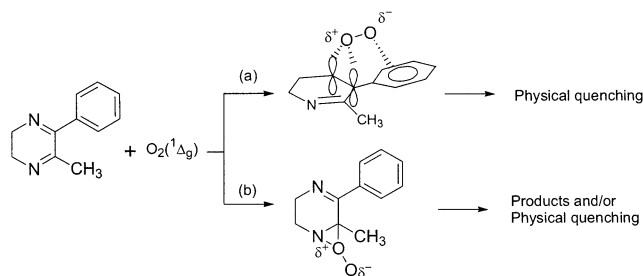
tions, dependence on the Hildebrand parameter is explained in terms of formation of an encounter complex of smaller molecular volume than the parent compounds. These reactions are also dependent on the dipolarity–polarizability parameter. Furthermore, examination of LSER and TLSER equations for MPD shows that the reaction is also assisted by HBA solvents and inhibited by HBD solvents. These results can be explained if phenyl substitution opens a further reactive channel in which the perepoxide is stabilized by interaction with the π system of a phenyl group such as proposed by Orfanopoulos et al.[4] to explain the solvent-dependent syn selectivity in reactions of $O_2(^1\Delta_g)$ with β,β-dimethylstyrene. A reaction mechanism compatible with our results is depicted in Scheme 3.

Reaction path a leads only to physical quenching through intersystem crossing to produce oxygen and the parent α-diimine. The geometry of the exciplex hinders the intramolecular hydrogen abstraction processes that stabilize it. The perepoxide shown in path a of Scheme 3 allows explanation of the observed solvent dependence. Decrease of the total reaction rate constants in HBD solvents can be understood in terms of interactions with the reactive center (the phenyl-substituted N–C double bond). Furthermore, an increase in sensitivity to HBA solvents may be due to electrostatic-stabilizing interactions with a positive charge on the complex. In addition, the dependence of k_T on the Hildebrand parameter is easily understand in terms of a phenyl group–perepoxide interaction. This interaction would be favorable in solvents with high cohesive energy, because interaction of negatively charged oxygen with the neighboring phenyl disrupts solvent–phenyl group interactions in the substrate. Furthermore, this hypothesis permits us to explain the low values of the chemical reaction constant measured for MPD even in polar solvents. As was mentioned above, the only reaction products detected were formaldehyde, 1-isocyano-2-(benzoylamino)ethane, and 1-isocyano-4-phenyl-4-carboxaldehyde-3-aza-3-butane, arising from singlet oxygen attack on a methyl-substituted N–C double bond, and the total reaction rate constant for this compound is at least 1 order of magni-

tude larger than for its dimethyl-substituted analogues. These data are consistent with the mechanism of sensitized photooxidation of MPD in Scheme 3. The increased reactivity of this compound toward singlet oxygen, relative to the dimethyl-substituted α-diimine, implies that the main path of reaction involves the interaction of O_2-$(^1\Delta_g)$ with the phenyl-substituted N–C double bond, to give a perepoxide-like exciplex that exclusively evolves by intersystem crossing due to there being no accessible α-hydrogen. Values of k_R relative to k_T are greatly reduced when comparing MPD results with DMD results in polar solvents. For DMD, k_R is very close to k_T, due to singlet oxygen interaction with the methyl-substituted N–C double bond to generate a perepoxide through path b, allowing possible hydrogen abstraction from a methyl substituent.

In conclusion, 5,6-disubstituted cyclic α-diimines are moderate to good singlet oxygen quenchers, being most effective in polar solvents. A reaction mechanism involving a perepoxide intermediate that evolves to a hydroperoxide from which products arise seems to be the main reaction path. Replacement of a methyl by a phenyl substituent opens an additional reaction path involving a perepoxide-like exciplex in which a stabilizing interaction of a negative charge on the free oxygen of a perepoxide with an aromatic π system contributes to the increased singlet oxygen quenching ability of cyclic α-diimines.

Experimental Section

5,10,15,20-Tetraphenyl-21H,23H-porphine (TPP), 9,10-dimethylanthracene (DMA), and 1,3-diphenylisobenzofurane (DPBF) were used without further purification. Rose Bengal (RB) was recrystallized twice from ethanol prior to use. All solvents were of spectroscopic or HPLC grade.

5,6-Dimethyl-2,3-dihydropyrazine (DMD) and 5-methyl-6-phenyl-2,3-dihydropyrazine (MPD) were synthesized as described;[34] typically a solution of 1-phenyl-2-propanedione (5 g) in ethyl ether (10 mL) was added to ethylenediamine (2 g) in 10 mL of ethyl ether maintained at 0 °C. The mixture was refluxed for 30 min and the ethereal yellow solution was dried over sodium sulfate and the solvent removed in a vacuum. The remaining yellow oil was cooled in a freezer during several hours, producing a solid from which pure 5-methyl-6-phenyl-2,3-dihydropyrazine was obtained as yellow needles by recrystallization from ethyl ether–hexane in 50% yield.

UV–vis absorption spectra and steady-state competitive kinetic experiments were performed. A GC–MS system with a Hewlett-Packard Ultra-2 capillary column (25 m) was used to obtain electron impact and chemical ionization mass spectra.

Chemical reaction rate constants were determined in several selected solvents using a 10 mL double-wall cell, light-protected by black paint. A centered window allowed irradiation with light of a given wavelength by using cutoff filters. Circulating water maintained the cell temperature at 22 ± 0.5 °C. Sensitizer irradiation (RB or TPP) was performed with a visible, 200 W, Par lamp. A gas chromatograph equipped with a NPD detector and a Hewlett-Packard Ultra-2 capillary column was used to monitor substrate consumption. DMA and DPBF were used as actinometers. Fresh DPBF solutions prepared in a dark room and appropriate cutoff filters were used. Autoxidation of this compound, followed by UV–vis spectrophotometry, was <1% under our experimental conditions.

(34) Flamet, I. F.; Stoll, M. *Helv. Chim. Acta* **1967**, *50*, 1754–1758.

Time-resolved luminescence measurements were carried out in 1 cm path fluorescence cells. TPP or RB were excited by the second harmonic (532 nm, nominal power 9 mJ per pulse) of a 6-ns light pulse of a Q-Switched Nd:YAG laser. A liquid nitrogen cooled germanium photodiode detector with a built-in preamplifier was used to detect infrared radiation from the cell. The detector was at a right-angle to the cell. An interference filter (1270 nm) and a cutoff filter (995 nm) were the only elements between the cell face and the diode cover plate. The preamplifier output was fed into the 1 MΩ input of a digitizing oscilloscope. Computerized experiment control, data acquisition, and analysis were performed with a LabView-based software developed in our laboratory.

Laser flash photolyses were performed with a Q-switched Nd:YAG laser (532 nm, ca. 35 mJ/pulse). A 150-W Xe lamp mounted in a lamp housing system was employed as monitoring light beam. The lamp beam was passed through a water filter before impinging on the entrance of the cell holder. An electronic shutter, controlled by a shutter driver/timer, was placed between the water filter and the cell holder. The shutter was triggered by the Q-switch from the laser. Two lenses and slits were used to collimate and focus the monitoring light to the cell holder and to the entrance slit of the monochromator. A photomultiplier detector mounted in a homemade housing was fitted to the monochromator exit slit port. PMT signals were monitored with a 500-MHz digital oscilloscope. An external PTI optical beam divider was employed to trigger the oscilloscope. The signals can be stored and averaged in the same scope at the repetition rate of the laser pulse (10 Hz) or can be fed to a personal computer equipped with home-designed software for data acquisition and treatment.

The determination of the total rate constants by steady-state competitive techniques in nonpolar solvents was done using the autoxidation rate of rubrene ($\lambda_{max} = 520$ nm).[22] The rate constants were obtained from the initial rate of rubrene consumption. In more polar solvents, TPP was employed as sensitizer ($\lambda_{max} = 414$ nm), and k_T values were determined by following the consumption of 9,10-dimethylanthracene upon addition of the dihydropyrazine derivative.[23] The irradiation was performed with a visible Par lamp (150 W) using a cutoff filter at 400 nm.

Equation coefficients and statistical parameters of LSER and TLSER correlations were obtained by multilinear correlation analysis with STAT VIEW 5.0 (SAS Institute Inc.). Results agreed with the t-statistic of descriptors.